



20th European Conference on Fracture (ECF20)

# The influence of hydrogen flux on crack initiation in martensitic steels

D. Guedes<sup>a,b</sup>, A. Oudriss<sup>a</sup>, S. Cohendoz<sup>a</sup>, J. Creus<sup>a</sup>, J. Bouhattate<sup>a</sup>, X. Feaugas<sup>a\*</sup>  
F. Thebault<sup>b</sup>, D. Koschel<sup>b</sup>

<sup>a</sup>LaSIE-CNRS FRE 3474, Université de La Rochelle, Avenue Michel Crépeau, 17042, La Rochelle, Cedex 0, France.

<sup>b</sup>Vallourec Research Center France, 60 route de Leval, F-59620 Aulnoye-Aymeries, France.

## Abstract

Understanding hydrogen transport and trapping phenomena is a key feature to revisit the hydrogen embrittlement (HE) models proposed in the literature. Both aspects can be affected by stress-strain states at different microstructural scales. Elastic distortion and plastic strain are both aspects of the mechanical states associated with defects (vacancies, dislocations), metallurgical elements (grain boundaries, precipitates), internal stresses and applied stresses, which can modify the diffusion and solubility of hydrogen. In the present work we first explore the effects of a tensile stress applied on martensitic steel membrane on the hydrogen concentration and mobility. In a second part, we analyse the impact of mobile and trapped hydrogen on HE using local approach of fracture under hydrogen flux.

© 2014 Published by Elsevier Ltd. Open access under [CC BY-NC-ND license](https://creativecommons.org/licenses/by-nc-nd/4.0/).

Selection and peer-review under responsibility of the Norwegian University of Science and Technology (NTNU), Department of Structural Engineering

*Keywords:* martensitic steel, hydrogen mobility, deep trapping of hydrogen, crack initiation, hydrogen embrittlement, local approach of fracture.

## 1. Introduction

The ductility and strength loss of quenched and tempered martensitic (QTM) steels has been clearly reported for high but also for low hydrogen contents. Despite the fact that some correlations exist between hydrogen embrittlement HE and hydrogen concentration and/or mechanical state, the HE mechanisms remains unclear. Indeed it is generally difficult to establish a relation between a complex microstructure and the different states of hydrogen (Wang *et al.* 2007, Tartaglia *et al.* 2008, Frappart *et al.* 2011, 2014). Thus it is complicated to establish a consensus on the impact of mobile and trapped hydrogen on damage mechanisms. In generally, it has been argued that a

segregation of hydrogen is necessary to reduce the interface energy and induce a cracking process (Hydrogen-Enhanced-Decohesion, HEDE). However, Wang has demonstrated recently that the cohesion energy was more lowered by mobile hydrogen than trapping hydrogen (Wang 2001). Moreover two other mechanisms have been proposed to explain HE. The improvement of vacancies formation by hydrogen solute (SAV: Super-Abundant Vacancies) promotes vacancies clustering and consequently the occurrence of damage. The reduction of the energy barrier on the dislocation motion through an elastic and/or an electronic shielding effect, promotes slip localization (HELP model associated with internal hydrogen: Hydrogen Enhanced Local Plasticity, or AIDE model associated with external hydrogen (adsorption), Adsorption Induced Dislocation Emission). In both cases, the distinction between diffusive or trapped hydrogen is not clearly established.

The structural heterogeneities in the martensitic microstructure are complexes. It can be easily modified through specific heat treatments (annealing, quenching and tempering). The choice of experimental parameters like the temperature or the exposure duration will mainly induce a modification of the size of prior  $\gamma$  grain, of the dislocation density and/or of the precipitation state. Weak variations of these parameters lead to particular properties in terms of hydrogen diffusion and HE resistance (Frappart *et al.* 2014). Thus the effect of hydrogen on crack initiation need to be considered at different microstructure scales (prior  $\gamma$  grains boundaries, lath, precipitate, inclusion, ...). To obtain more accurate results on HE of QTM steels, it is important to develop a specific experimental approach, which allows distinguishing the impact of the different states of hydrogen on the occurrence of damage at different microstructural scales.

The main goal of this study is to introduce a new experimental method to strength a material until fracture under hydrogen flux applied duringg an electrochemical permeation test.

### Nomenclature

QTM	Quenched Tempered Matensitic steel
HE	Hydrogen Embrittlement
HEDE	Hydrogen Enhance Decohesion
HELP	Hydrogen Enhanced Local Plasticity
AIDE	Adsorption Induced Dislocation Emission
SAV	Super-Abundant Vacancies
TDS	Thermal Desorption Spectroscopy

## 2. Material and experimental device

The studied alloys are quenched and tempered Fe-nC-mX martensitic steels (QTM) with a chemical composition given by n between 0.3 to 0.4 wt% and m between 0.003 to 1.2 wt% of  $X \in \{\text{Cr, Mn, Mo, Ni, P, S, Cu, Al, V, Nb, As, Co}\}$ . The alloys are first annealed at a temperature above 1130 K during 20 min and then baked between 670 K to 980 K during 20 to 30 min. Large experimental investigations have been performed recently to obtain an average description of the microstructure in terms of precipitate state, dislocation density, inter-lath density and prior austenitic grain size. The details of these results and the experimental procedures of each techniques used for these investigations are reported in our previous works (Frappart *et al.* 2010, 2012, 2014). Martensite is the main phase with prior-austenite grains (grain size between 10 to 30  $\mu\text{m}$ ), composed of one or more variants of martensite. Coarse second-phase particles imbedded in martensitic matrices as inclusions, (fraction of 55  $\text{mm}^{-2}$ ) consist essentially of spherical aluminum oxide  $\text{Al}_2\text{O}_3$  (diameter of 5  $\mu\text{m}$ ). The dislocations density is high in the intra-laths area. This density is of the order of  $2.84 \cdot 10^{14} \text{ m}^{-2}$  (evaluated by TEM), which is a value greater than the mean dislocations density required to accommodate the misorientations between laths of  $1.3 \cdot 10^{14} \text{ m}^{-2}$  (determined by SEM-EBSD). At nanometer scale, we observed a fine carbide precipitation (a radius of 20 nm with a fraction lower than 1%).

Mechanical experiments were performed using a fatigue testing device INSTRON 100 kN with a strain rate of  $10^{-5} \text{ s}^{-1}$ . Tensile tests were carried out on equiaxed V-notch samples and prismatic samples with or without V-notch.

The notch specimens are designed to obtain an average stress concentration factor  $K_t=3.16$ . Equiaxed V-notch samples are pre-charged at a constant charging current density ( $20 \text{ mA/cm}^2$ ) in  $1\text{M H}_2\text{SO}_4$  during 24h. The total hydrogen content measured by TDS (Thermal Desorption Spectroscopy) is around 1.5 wppm with a contribution of hydrogen deep trapped equal to 0.7 wppm. To perform electrochemical permeation (EP) tests under stress, a specific design of experimental device has been developed in our laboratory (Frappart *et al.* 2012). A prismatic tensile sample was assembled with the permeation device. At the beginning, the detection side of the sample was potentiostatically maintained at a constant potential in  $0.1 \text{ M NaOH}$  during 22h in order to stabilize the anodic current to around  $0.1 \mu\text{A/cm}^2$ . Then the entry side of the specimen was galvanostatically polarized at a constant charging current density ( $20 \text{ mA/cm}^2$ ) in  $1\text{M H}_2\text{SO}_4$  and the hydrogen flux was measured on the exit side during the sorption step until that a steady state was reached. Solutions in both cells were continuously deoxygenated with argon. Three kinds of tensile tests have been performed for prismatic specimen without notch: (i) without hydrogen charging steps, (ii) under hydrogen flux during steady state and (iii) after a sequence of sorption-desorption. For the last one, after the sorption step the charging current density was stopped, the acid solution was then released from the charging cell and the deaeration with argon was maintained. So the desorption step was recorded. The complete decay is sensitive to the hydrogen release and it is used to evaluate the amounts of lattice and trapped hydrogen as described in literature (Frappart *et al.* 2010, Oudriss *et al.* 2012). The aim of this method is to separate lattice from trapped hydrogen concentrations by comparing both experimental and theoretical curves deduced from Fick diffusion laws. At the end of this step only irreversible trapped hydrogen stays in the material (Frappart *et al.* 2011). For the prismatic sample with notch, only tensile test under hydrogen flux at steady state have been performed. At the end of each test, hydrogen content has been measured near fracture surface using TDS.

### 3. Results and discussion

The results of this study will be presented in two parts, first we expose the impact of the mechanical state on hydrogen flux and then we demonstrate the impact of diffusive and trapped hydrogen on the loss of ductility.

#### 3.1. Impact of stress-strain states on hydrogen flux

The effect of stress-strain state on hydrogen flux is illustrated on figure 1. For a prismatic specimen strengthened at a constant strain rate ( $10^{-5} \text{ s}^{-1}$ ) under hydrogen flux at steady-state, we observe different regimes. In the elastic domain, as it was previously reported (Frappart *et al.* 2012, Guedes *et al.* 2014), the hydrogen flux increases with the applied stress. We previously showed that applied elastic stresses influence mainly the lattice concentration. In the thermodynamic framework, the solid submitted to an elastic stress field may accommodate more interstitial hydrogen due to the elastically expanded lattice (Li *et al.* 1966, Bech *et al.* 1966, Kirchheim 1982, Larche *et al.* 1985, Frappart *et al.* 2012). More precisely, the elastic stress affects the hydrogen solubility, which can be related to the hydrostatic stress  $\sigma_m$  interactions with the partial molar volume of hydrogen. We have recently showed that vacancies clusters can be contributed to this interaction (Guedes *et al.* 2014a, 2014b). During the development of Lüders bands the stress and the flux remain constant. When the plastic strain occurs locally under the hydrogen flux, we observed a large increase of the hydrogen flux. This result demonstrates that hydrogen transport is assisted by mobile dislocations in agreement with the contributions of Chêne *et al.* (1999) and Shoda *et al.* (2010). Above a critical value of plastic strain, the hydrogen flux decreases as a function of plastic strain. According to Lan's *et al.* (1992) work on ferritic steels, at the earlier stage of plastic strain, the density of mobile dislocations rapidly increases to reach a stationary regime in which dislocations clusters and dislocation cells are formed. Then the density of storage dislocations in the material increases. Consequently, we can correlate the decrease of hydrogen flux to the increase of deep trapped sites associated with the core of storage dislocation density.

Present results illustrates clearly the competition between mobile dislocation and storage dislocation. The first one promote the transport of hydrogen and second one leads to an increase of the trapping process. Both aspects must be taken into account to describe a realistic interaction between plasticity and hydrogen.

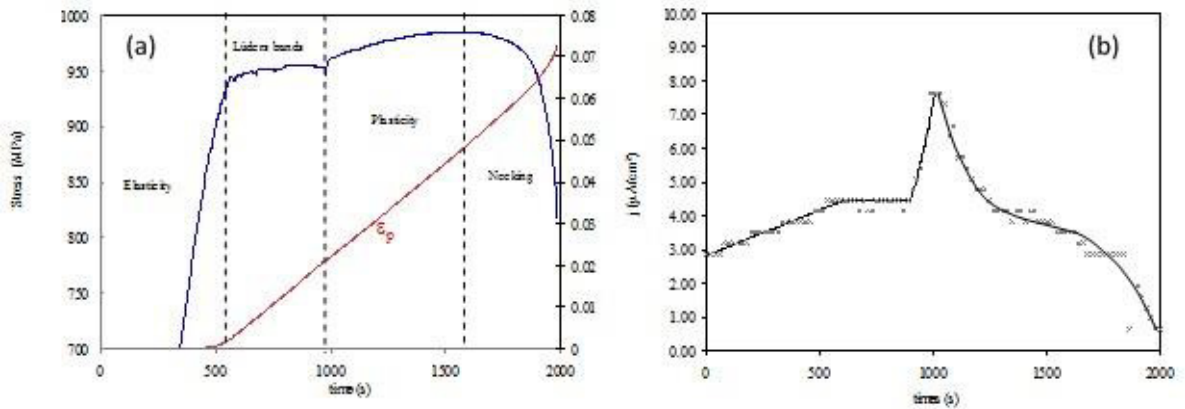


Fig. 1. (a) Stress and plastic strain  $\epsilon_p$  versus time; (b) hydrogen flux versus time.

### 3.2. Impact of diffusive and trapped hydrogen on the ductility

First we consider the hydrogen pre-charged axisymmetric specimens (figure 2a). It appears clearly that for a concentrations of irreversible trapped hydrogen below 0.7 wppm, there is no effect on the mechanical behavior of V-notch specimens. Similar results were obtained for specimen without a notch. Thus this result does not seem to depend on stress concentration factor. However, when the mechanical test is performed under hydrogen flux we observe a clearly loss of ductility. Additionally, the applied stress promotes the apparent hydrogen solubility equal to 2.7 wppm versus 1.5 wppm for the same charging condition without stress. Consequently, we can conclude that the diffusive hydrogen seems to promote hydrogen embrittlement more than the trapped hydrogen. The observations of the fracture surface illustrate the fact that trapped hydrogen has no effect on the ductile fracture process (figure 3a).

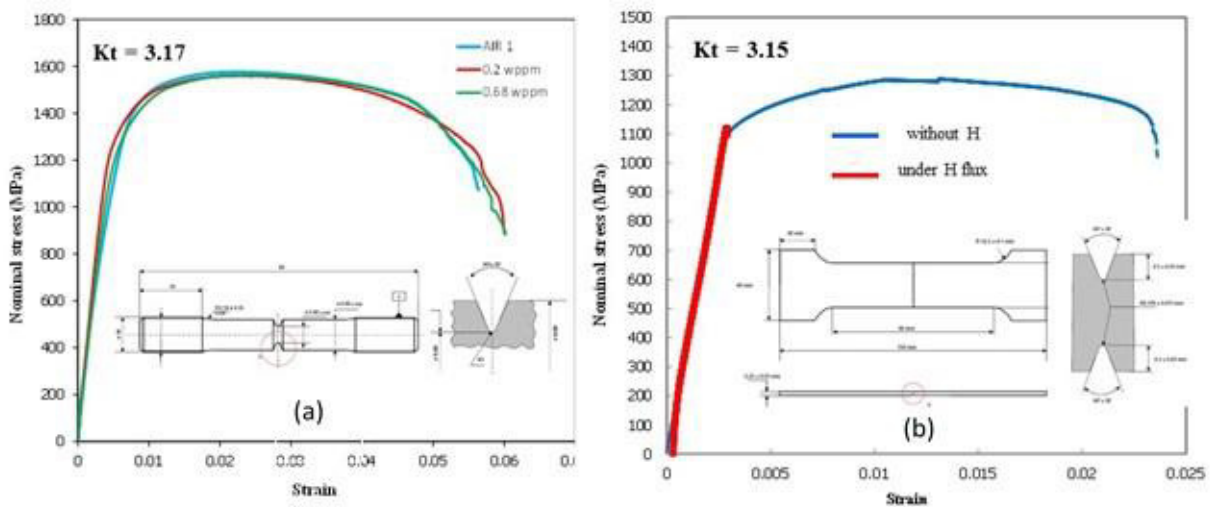


Fig. 2. (a) Stress versus strain with pre-charging in hydrogen (only irreversibly trapped hydrogen); (b) Stress versus strain for prismatic sample with or without hydrogen flux.

Scanning electronic images of the fracture surface after tensile testing of the pre-charged specimen exhibit ductile decohesion, typical of a large density of small dimples associated with carbides and some large dimples resulting to decohesion and growth of damage around inclusions ( $\text{Al}_2\text{O}_3$ ). In opposite, the diffusive hydrogen promote quasi-cleavage at a microstructural scale, which corresponds to martensitic laths. This last result has been recently reported by our group (Oudriss *et al.* 2014) in the specific case of the impact of hydrogen degasing on the tensile ductility of QTM steels. In that case, the minimum of ductility observed corresponds to a quasi-cleavage process at laths scale and a maximum of hydrogen mobility.

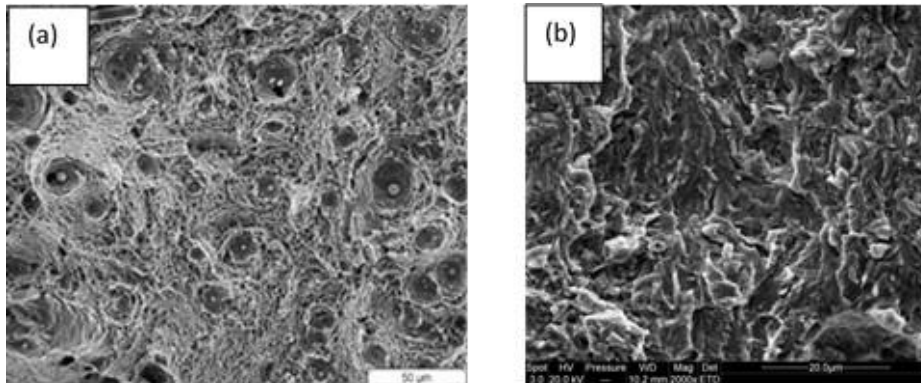


Fig. 3. Fracture surface in process zone for (a) axisymmetric notch pre-charged specimen and for (b) prismatic sample strained under hydrogen flux.

#### 4. Conclusions

The effect of hydrogen content and mobility on damage has been investigated for different mechanical states. We show the importance to consider the different impact of the plasticity on diffusive hydrogen and trapped hydrogen. The last one does not seem to impact the ductility. In opposite diffusive hydrogen induce a quasi-cleavage process at the martensitic laths scale.

#### References

- Beck W., Bockris J.O'M., McBreen J., Nanis L., Proc. R. Soc. Lond. A 290 (1966) 220–235.  
 Chêne J., Brass AM., Scripta Met. 40, n°5 (1999) 537.  
 Frappart S., Feaugas X., Creus J., Thebault F., Delattre L., Marchebois H., J. Phys. Chem. Solids 71 (10) (2010) 1467–1479.  
 Frappart S., Oudriss A., Feaugas X., Creus J., Bouhattate J., Thébault F., Delattre L., Marchebois H., Scr. Mater., 65 (2011) 859–862.  
 Frappart S., Feaugas X., Creus J., Thebault F., Delattre L., Marchebois H., Mater. Sci. Eng. A 534 (2012) 384–393.  
 Frappart S., Feaugas X., Conforto E., Creus J., Thebault F., Delattre L., Marchebois H., Metall. Mater. Trans. A (2014) in revision.  
 Guedes D. *et al.*, Scripta Mater. In progress 2014.  
 Kirchheim R., Acta Metall. 30 (1982) 1069–1078.  
 Lan Y., Klaar HJ, Dahl W., Metall. Trans. A 23 (1992) 537.  
 Larche F.C., Cahn J.W., Acta Metall. 33 (1985) 331–357.  
 Li J.C.M., Oriani R.A., Darken L.S., Physik Z., Chem. 49 (1966) 271–290.  
 Oudriss A., Creus J., Bouhattate J., Conforto E., Berziou C., Savall C., Feaugas X., Acta Mater. 60 (2012) 6814.  
 Oudriss A. *et al.*, Mat. Sci. Eng. A, (2014) to be published.  
 Shoda H. *et al.*, ISIJ International, 50 (2010) 115–123.

Tartaglia J. M., Lazzari K. A., Hui G. P., Hayrynen K. L., *Metall. Mater. Trans. A.*, 39 (2008) 559-576.  
Wang M., Akiyama E., Tsuzaki K., *Corr. Sci.*, 49 (2007) 4081–4097.  
Wang J.S., *Eng. Frac. Mech.*, 68 (2001) 647-669